

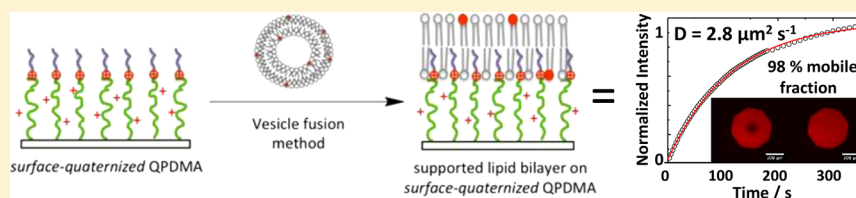
Facile Formation of Highly Mobile Supported Lipid Bilayers on Surface-Quaternized pH-Responsive Polymer Brushes

N. Cheng,[†] P. Bao,[‡] S. D. Evans,[‡] G. J. Leggett,[†] and S. P. Armes^{*,†}

[†]Department of Chemistry, University of Sheffield, Sheffield S3 7HF, U.K.

[‡]Molecular and Nanoscale Physics Group, School of Physics and Astronomy, University of Leeds, Leeds LS2 9JT, U.K.

S Supporting Information



ABSTRACT: Poly(2-dimethylamino)ethyl methacrylate (PDMA) brushes are grown from planar substrates via surface atom transfer radical polymerization (ATRP). Quaternization of these brushes is conducted using 1-iodooctadecane in *n*-hexane, which is a non-solvent for PDMA. Ellipsometry, AFM, and water contact angle measurements show that surface-confined quaternization occurs under these conditions, producing pH-responsive brushes that have a hydrophobic upper surface. Systematic variation of the 1-iodooctadecane concentration and reaction time enables the mean degree of surface quaternization to be optimized. Relatively low degrees of surface quaternization (ca. 10 mol % as judged by XPS) produce brushes that enable the formation of supported lipid bilayers, with the hydrophobic pendent octadecyl groups promoting *in situ* rupture of lipid vesicles. Control experiments confirm that quaternized PDMA brushes prepared in a good brush solvent (THF) produce non-pH-responsive brushes, presumably because the pendent octadecyl groups form micelle-like physical cross-links throughout the brush layer. Supported lipid bilayers (SLBs) can also be formed on the non-quaternized PDMA precursor brushes, but such structures proved to be unstable to small changes in pH. Thus, surface quaternization of PDMA brushes using 1-iodooctadecane in *n*-hexane provides the best protocol for the formation of robust SLBs. Fluorescence recovery after photobleaching (FRAP) studies of such SLBs indicate diffusion coefficients ($2.8 \pm 0.3 \mu\text{m}^2 \text{s}^{-1}$) and mobile fractions ($98 \pm 2\%$) that are comparable to the literature data reported for SLBs prepared directly on planar glass substrates.

INTRODUCTION

There has been substantial interest in stimulus-responsive polymers for at least the past two decades.^{1–5} Typical stimuli include changes in pH,^{6–9} temperature,^{10–14} light,¹⁵ and electrolyte concentration,^{16–18} and such responsive polymers offer potential applications in many areas, including biomedical sensing,^{3,19–21} lubrication,²² and electronic devices.^{23–25} One of the most studied examples is pH-responsive polymers. For example, weak polyacids and polybases generally exhibit pH-responsive behavior: ionization or protonation of the side chains of vinyl polymers can cause either chain extension or chain collapse in aqueous solution.

A polymer brush has at least one end tethered to a surface.²⁶ Brushes can be readily grown from either planar^{27–31} or colloidal^{32–35} surfaces using living radical polymerization techniques.^{36–38} In particular, brushes based on weak polyelectrolytes such as poly(methacrylic acid)^{39,40} have been designed to act as pH-selective membranes,⁴¹ pH-triggered actuators,⁴² and pH-controlled chemical gates.^{39,40,43–45} One of the most studied classes of pH-responsive brushes are amine-functional polybases such as poly[2-(dimethylamino)ethyl methacrylate] (PDMA),^{7,46,47} poly[2-(diethylamino)ethyl methacrylate] (PDEA),^{48–50} poly[2-(diisopropylamino)ethyl

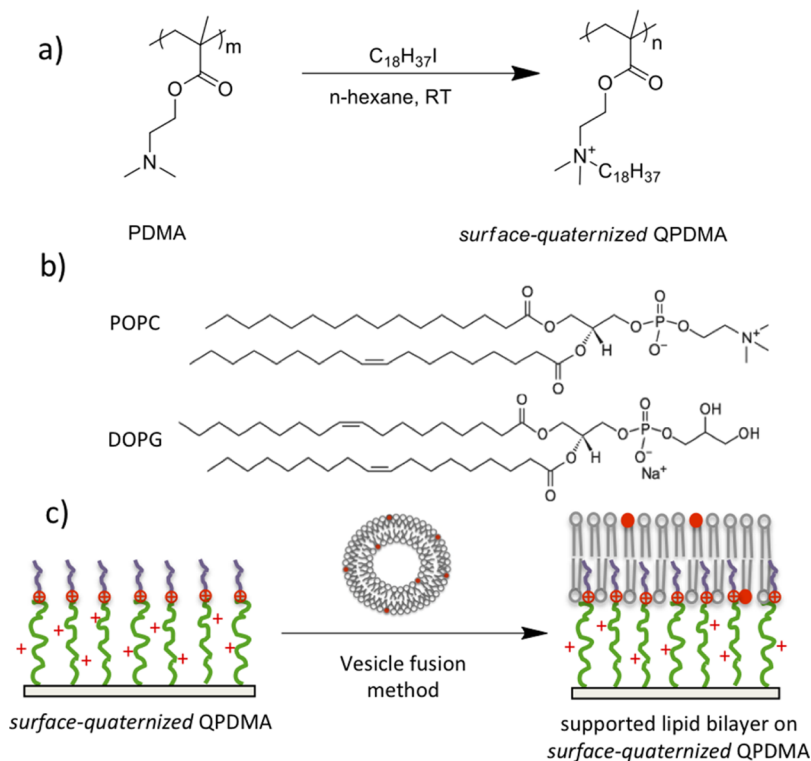
methacrylate] (PDPA),^{48,51,52} and 2-(*tert*-butylamino)ethyl methacrylate (PTBAEMA).^{53,54} In particular, Murata et al.⁵⁵ grew PDMA brushes from a planar surface via surface-initiated atom transfer radical polymerization (ATRP) and subsequently quaternized these chains with various alkyl bromides. The resulting cationic surfaces exhibited high antimicrobial activity, with a strong correlation being observed between efficacy and surface charge density. Similarly, Cheng et al.⁵⁶ reported that quaternized PDMA brushes exhibited useful bactericidal properties. In this case PDMA brushes were grown from cross-linked poly(4-vinylbenzyl chloride) microspheres and then quaternized using either 1-bromododecane or 1-bromohexane. The resulting cationic brushes proved effective against *E. coli* and *S. aureus*. Dong et al.⁵⁷ also prepared cationic brushes, but in this case 2-(methacryloyloxy)ethyl]-trimethylammonium chloride was polymerized directly in aqueous solution, so no post-polymerization quaternization step was required. Patterning such brushes using photolithography produced well-defined cationic surface patterns

Received: March 2, 2015

Revised: April 2, 2015

Published: April 16, 2015

Scheme 1. (a) Schematic Representation of a Surface-Quaternized QPDMA Brush Obtained after Reacting a PDMA Precursor Brush with 1-Iodoctyldecane in *n*-Hexane at 20 °C; (b) Chemical Structures of 1-Palmitoyl-2-oleoyl-*sn*-glycero-3-phosphocholine (POPC) and 1,2-Dioleoyl-*sn*-glycero-3-phospho-(1'-*rac*-glycerol) (DOPG) Lipids; (c) Schematic Representation of the Formation of a Supported Lipid Bilayer (SLB) on the Resulting Surface-Quaternized Partially Protonated QPDMA Brush Layer via the Vesicle Fusion Method^a



^aThe PQDMA brush-coated substrate was incubated with a lipid vesicle suspension comprising 89.5 mol % POPC, 10 mol % DOPG, and 0.5 mol % TR-DHPE fluorescent dye in PBS buffer (pH 7.4) at 50 °C for 1 h, rinsed with deionized water, and then further incubated in a pH 8.7 buffer solution containing 1 M KCl and 100 mM K_2HPO_4 at 50 °C for 16 h.

that allowed excellent spatial control to be achieved for the growth of rat hippocampal neurons.

We recently reported the synthesis of secondary amine-functionalized PTBAEMA brushes from a planar surface via ATRP.⁵⁴ By reacting a commercially available polymeric diisocyanate with the brush chains immersed in a good solvent (THF) or a bad solvent (*n*-hexane), either uniform cross-linking or surface cross-linking could be achieved. Moreover, the behavior of the resulting brushes was strongly dependent on the spatial location of the cross-linking reaction: the surface cross-linked PTBAEMA brush exhibited a stronger pH response than the uniformly cross-linked PTBAEMA brush, as judged by ellipsometry and AFM studies.

There has been considerable recent interest in the design and synthesis of supported lipid bilayers (SLBs).^{58–66} In principle, a high-quality SLB confers high lipid mobility and conformational flexibility.⁶⁷ Lipid bilayers have been deposited onto various neutral, zwitterionic, or polyelectrolytic brushes. For example, Wirth and co-workers⁶⁵ placed POPC lipid bilayers on polyacrylamide brushes of 10 nm thickness grown by surface ATRP in DMF at room temperature. Similarly, a 16 nm zwitterionic polysulfobetaine polymer was grown via surface ATRP by Vancso et al.,⁶⁴ who found that bilayer deposition could be controlled by varying the brush graft density; lipid diffusion coefficients of approximately $1 \mu m^2 s^{-1}$ were reported using this approach. Renner and co-workers⁶³ grafted a pH-responsive maleic anhydride-based copolymer onto an amine-

functionalized planar surface to support bilayer formation, with electrostatic interactions being modulated by conducting lipid deposition at pH 4. However, such acidic conditions are likely to promote protein denaturation. Similarly, poly(diallyldimethylammonium chloride) has been grafted onto a planar substrate by Tang et al., who then deposited highly anionic lipid vesicles onto this cationic polyelectrolyte layer.⁶⁶ A weakly anionic statistical copolymer brush composed of *N*-isopropylacrylamide and acrylic acid has also been evaluated as a membrane support, with bilayer formation being achieved when using vesicles comprising a binary mixture of cationic and zwitterionic lipids.⁶¹ Polyelectrolyte multilayers have also been utilized by various workers to produce suitable cushions that promote bilayer deposition.^{58–60,62} In some cases, pH-responsive cushions were reported.⁵⁹

Various non-ionic polymeric cushions based on poly(ethylene glycol) (PEG),^{68–71} cellulose,⁷² or dextran⁷³ have been reported to be suitable for the formation of SLBs. In addition, El-Khoury et al.⁷⁴ demonstrated that an anionic poly(acrylic acid) (PAA) cushion could serve as a suitable substrate for the formation of supported membranes. In this case, the pH-responsive nature of the PAA chains enabled the measurement of proton transport across the membrane. Very recently, we have shown that a new zwitterionic poly(amino acid methacrylate) brush comprising cysteine side groups⁷⁵ can also be used for SLB applications.⁷⁶

In the present study, we explore the post-synthesis modification of ATRP-synthesized PDMA brushes grown from a planar surface.^{77–79} This is achieved via reaction with 1-iodooctadecane in *n*-hexane, which is a non-solvent for the brush chains. This unusual approach ensures that quaternization is *surface-confined*, which is essential for the design of a pH-responsive brush with sufficient near-surface hydrophobic character to enable the formation of an SLB (see Scheme 1a). In principle, simply varying the 1-iodooctadecane concentration should provide control over the mean degree of surface quaternization. Moreover, *in situ* ellipsometry and AFM studies are used to characterize the pH responsive behavior of these surface-quaternized brushes (denoted QPDMA), which is compared to that of the original PDMA brush and also a QPDMA brush in which quaternization is conducted in a good brush solvent (THF). Finally, FRAP measurements are used to assess the quality of the SLBs formed on surface-quaternized QPDMA brushes using the vesicle fusion method.⁸⁰

EXPERIMENTAL SECTION

Materials. Silicon wafers ([100] orientation, boron-doped, 0–100 Ω cm) were purchased from Compant Technology (Peterborough, UK). Deionized water was obtained using an Elga Pure Nanopore 18.2 M Ω system. 3-Aminopropyltriethoxysilane (APTES) (>98%), 2-bromoisobutyl bromide (BIBB) (98%), and triethylamine (99%) were purchased from Sigma-Aldrich (Gillingham, UK). Hydrogen peroxide (30%), sulfuric acid (95%), ethanol (99.8%, HPLC grade), ammonium hydroxide (Analar), dichloromethane (HPLC grade), *n*-hexane (HPLC grade), DMF (HPLC grade), THF (HPLC grade), and basic alumina were obtained from Fisher Scientific (Loughborough, UK). Copper(I) bromide (>98%), 1,1,4,7,10,10-hexamethyltriethylenetetramine (HMTETA, 97%), 1-iodooctadecane (95%), and 2-(dimethylamino)ethyl methacrylate (DMA, 98%) were obtained from Sigma-Aldrich (Gillingham, UK). α -Bromobutyrate-11-undecanethiol was purchased from Prochimia (Poland). 1-Palmitoyl-2-oleoyl-*sn*-glycero-3-phosphocholine (POPC, 99%) and 1,2-dioleoyl-*sn*-glycero-3-phospho-(1'-*rac*-glycerol) (DOPG, 99%) lipid were purchased from Avanti Polar Lipids Inc. (Alabaster, AL). Texas Red-modified 1,2-dihexadecanoyl-*sn*-glycero-3-phosphoethanolamine (TR-DHPE, 99%) was purchased from Invitrogen Ltd. (Paisley, UK). All chemicals were analytical reagent grade and were used as received. Copper(I) bromide was stored under vacuum prior to use. DMA was treated with basic alumina to remove inhibitor and stored at 4 °C before use.

Preparation of ATRP Initiator on Silicon Wafers. All glassware and substrates were immersed in piranha solution for 2 h. (*Caution: piranha solution comprises three parts hydrogen peroxide to seven parts concentrated sulfuric acid; it is an extremely strong oxidizing agent that has been known to detonate spontaneously upon contact with organic material.*) The piranha-treated glassware and the substrates were rinsed copiously with deionized water and then sonicated for 10 min, followed by oven-drying at 120 °C for 1 h. These clean silicon/glass wafers were then immersed in a 1:1:5 solution of ammonium hydroxide, 30% hydrogen peroxide, and deionized water. This reaction solution was heated to 85 °C for 30 min before being allowed to cool to 20 °C. The treated wafers were rinsed with deionized water, sonicated, and then oven-dried prior to use.^{81,82} A 2.0% v/v ethanolic solution of 3-aminopropyltriethoxysilane (APTES) was aged for 5 min at 20 °C. Silicon/glass wafers were immersed in this APTES solution for 30 min, then rinsed with ethanol, dried using a nitrogen gas stream, and annealed for 30 min at 120 °C.^{81–83} The resulting surface-initiated wafers were then immersed in a solution of 2-bromoisobutyl bromide (BIBB) (0.37 mL, 3 mmol) and triethylamine (0.41 mL, 3 mmol) in dichloromethane (60 mL) for 30 min at 20 °C. Subsequently, the initiator-functionalized wafers were rinsed with ethanol and dichloromethane, followed by drying using a nitrogen gas stream prior to use. The same protocol was used for the growth of

PDMA brushes on gold, except that the surface polymerizations were conducted at 40 °C.

Preparation of ATRP Initiator on Gold-Coated Wafers. Planar gold substrates were prepared on silicon wafers using an Auto 306 thermal evaporator (BOC Edwards). First, a 15 nm chromium layer was deposited onto a piranha solution-treated planar silicon wafer at a rate of 0.1 nm s⁻¹, followed by deposition of a 200 nm gold layer under the same conditions. Gold-coated wafers were rinsed with ethanol and dried under a N₂ stream. A SAM monolayer of α -bromobutyrate-11-undecanethiol was prepared by immersing the gold-coated wafer into a 5 mM ethanolic solution of this ATRP initiator overnight. The wafer was subsequently removed from the reaction solution and washed with ethanol to remove excess initiator prior to drying under N₂.

Photopatterning of ATRP Initiator-Functionalized Surfaces. A Coherent Innova 300C FreD frequency-doubled argon ion laser (Coherent UK, Ely, UK) was used to irradiate samples at a UV wavelength of 244 nm. The laser power was adjusted over the 1–100 mW range. The area exposed to the laser beam was 0.06 cm². Micropatterns were obtained by irradiation of the 3-(2-bromoisobutyramido)propyltriethoxysilane (BIBAPTES) monolayer on the silicon/glass wafer using a 2000 mesh electron microscope copper grid (Agar, Cambridge, UK) as a convenient mask.^{81,83} More specifically, micropatterning was achieved by exposing BIBAPTES-functionalized silicon wafers to 10 J cm⁻² laser radiation at 244 nm for 2–10 min depending on the laser power. This protocol ensures complete removal of Br atoms in the irradiated areas.⁸¹ Atomic force microscopy (AFM) was used to image the resulting surface patterns.

ATRP Synthesis of PDMA Brushes. DMA (47.1 g, 30 mmol) was dissolved in DMF (50 mL), deoxygenated for 20 min, and stored under N₂ prior to use. HMTETA (0.30 mL, 0.15 mmol) was added to the solution and deoxygenated for 10 min, after which Cu(I)Br (0.14 g, 0.10 mmol) was added and the monomer/catalyst mixture was deoxygenated for a further 10 min. Initiator-coated wafers were sealed in Schlenk tubes and deoxygenated via three vacuum/nitrogen cycles. The monomer/catalyst solution (5.0 mL) was syringed into each tube under a nitrogen atmosphere, and the surface polymerization of DMA was allowed to proceed at 90 °C for the desired reaction time. Each polymerization was quenched by removing the wafer from its Schlenk tube, followed by washing with IPA and ethanol several times to remove excess monomer and catalyst. The same protocol was used for the synthesis of micropatterned PDMA brushes.

Quaternization of PDMA Brushes in *n*-Hexane. 1-Iodooctadecane solutions ranging in concentration from 0.1 to 200 μ M were prepared freshly in 10 mL of *n*-hexane before use. PDMA brush-coated wafers prepared as described above were cut into small pieces (\sim 1 cm²) and immersed in various 1-iodooctadecane solutions for approximately 18 h at 20 °C. The resulting *surface-quaternized* PDMA brushes (denoted “QPDMA”) were then rinsed using *n*-hexane, ethanol, and acetone, with further sonication in *n*-hexane for 10 min followed by drying under a stream of N₂ gas. Contact angle measurements, ellipsometric studies, and XPS analyses were performed on each QPDMA brush-coated wafer.

Quaternization of PDMA Brushes in THF. A 100 μ M solution of 1-iodooctadecane in 10 mL of THF was freshly prepared before use. PDMA brush-coated silicon wafers (prepared as described above) were cut into small pieces (\sim 1 cm²) and immersed in this 1-iodooctadecane solution for approximately 18 h at 20 °C. The resulting *uniformly quaternized* PDMA brushes were then rinsed using THF, ethanol, and acetone, followed by sonication in THF for 10 min and finally dried under a stream of N₂ gas.

Preparation of Lipid Vesicles. A 1.0 mg lipid mixture comprising 89.5 mol % POPC, 10 mol % DOPG, and 0.5 mol % TR-DHPE was codissolved in a 1:1 v/v chloroform/methanol mixture. This lipid solution was dried under nitrogen flow for 30 min and then in a desiccator under vacuum (0.1 mbar) for 12 h to remove all traces of solvent. The dried lipid mixture was subsequently resuspended in phosphate buffered saline (PBS) buffer (1.0 mL) to give a final lipid solution concentration of 1.0 g dm⁻³. Small unilamellar vesicles (SUVs) were produced by the tip-sonication method (30 min at 4

°C), using a Branson sonifier (Branson Ultrasonics Corp., Danbury, CT). The resulting suspension was centrifuged for 1 min at 14 500 rpm in order to remove any residual particles deposited by the tip. The supernatant was diluted with PBS to give a final concentration of approximately 0.50 g dm^{-3} . This stock solution was then used immediately or stored in a refrigerator at $4 \text{ }^\circ\text{C}$ for up to a few days prior to use.

Lipid Bilayer Formation on QPDMA Brushes. A QPDMA brush-coated 18 mm diameter round glass disk was incubated with the SUV suspension described above for 1 h at $50 \text{ }^\circ\text{C}$ using a home-built flow cell.⁸⁴ After being rinsed with deionized water at a flow rate of 1.50 mL min^{-1} for 30 min, a supported lipid bilayer (SLB) was formed on the QPDMA brush surface. To enhance its stability and fluidity, this SLB structure was incubated in a pH 8.7 buffer solution (comprising 1 M KCl and 100 mM K_2HPO_4) for 16 h at $50 \text{ }^\circ\text{C}$.

Surface Characterization. Ellipsometric studies were conducted using an Alpha-SE ellipsometer (J.A. Woollam Co., Lincoln, NE) equipped with a He-Ne laser ($\lambda = 633 \text{ nm}$) at an incident angle (Φ) of 70° from the normal. Mean brush thicknesses were calculated from silicon substrate models. Measurements were conducted from 300 to 700 nm, and modeling was performed using WVASE software (J.A. Woollam Co., Lincoln, NE). The fit quality was assessed using the root-mean-square error (RMSE) between the measured and modeled ellipsometric constants Δ and Ψ over all measured wavelengths. The dry films were modeled as a single layer of variable thickness, with a refractive index given by the Cauchy parameters of $A_n = 1.5 \mu\text{m}^2$ and $B_n = 0.005 \mu\text{m}^2$ (determined by fitting these values to data obtained for a PDMA brush of 35 nm dry thickness). The ellipsometric brush thickness for each sample was determined in at least three different positions on each wafer and reported as the mean \pm standard error.⁵¹ *In situ* measurements of brush thickness in aqueous solution were conducted using a homemade liquid cell. The sample cell was rinsed several times with deionized water between each measurement. Ellipsometric data were fitted using a single slab model with a refractive index given by a linear effective medium approximation (EMA) between the PDMA or QPDMA brush and water.^{48,85} Again, three measurements were recorded for each brush-coated wafer, and data are reported as the mean \pm standard error.

AFM measurements were conducted using a Digital Instruments Nanoscope IV multimode atomic force microscope (Veeco, Santa Barbara, CA) equipped with a "J" scanner ($0\text{--}125 \mu\text{m}$). Silicon nitride nanoprobes (Digital Instruments, Cambridge, UK) with nominal spring constants ranging from 20 to 80 N m^{-1} were used for tapping mode imaging. All samples were allowed to stand in the liquid cell for at least 5 min prior to any measurements in order to attain equilibrium. Mean heights were determined both for dry micro-patterned brushes in air and for swollen brushes immersed in aqueous solutions of various pH buffers ranging from pH 2 to pH 11.

X-ray photoelectron spectroscopy (XPS) studies were conducted using a Kratos Axis Ultra spectrometer (Kratos Analytical, Manchester, UK) equipped with a monochromatic Al $K\alpha$ X-ray source operating at a power of 150 W with an emission current of 8 mA. The base pressure in the spectrometer was typically $10^{-8}\text{--}10^{-10}$ mbar. Electron energy analyzer pass energies of 20 and 160 eV were used to acquire core-line spectra and survey scans, respectively. The energy resolution for the wide scans was 1.0 eV. This was reduced to 0.1 eV for high-resolution scans. Core-line spectra were peak-fitted using Casa XPS software, and all binding energies were referenced relative to the main hydrocarbon C 1s signal calibrated at 285 eV.

Fluorescence recovery after photobleaching (FRAP) data were recorded using an epifluorescence microscope (E300 Nikon, USA). The sample was illuminated and bleached using a high-pressure mercury arc lamp. The bleached spot had a diameter of $28 \mu\text{m}$ as viewed using a $\times 40$ objective lens. After bleaching, a series of time-lapse fluorescence images were collected using a Zyla sCMOS CCD camera (Andor Technology Ltd. Belfast, UK) with the aid of NIS elements software (Nikon, USA). The Axelrod method was employed to calculate the diffusion coefficient and the mobile fraction of the supported lipid bilayer.⁵¹

RESULTS AND DISCUSSION

Selective quaternization has been previously reported by Bütün et al.,⁸⁶ who prepared a range of near-monodisperse tertiary amine methacrylate-based diblock copolymers via group transfer polymerization. In the case of PDMA–PDEA and PDMA–PDPA diblock copolymers, remarkably selective quaternization of the more reactive PDMA block was observed, provided that the quaternization reagent (e.g., methyl iodide or benzyl chloride) was not used in excess relative to the DMA residues. In the present work, selective *surface* quaternization of PDMA brushes is achieved by selecting a poor solvent for the PDMA chains. This means that quaternization is conducted on the collapsed brush rather than on the extended brush, which ensures that derivatization is confined to the brush extremities. This approach is essential to ensure that the brush retains its pH-responsive character (see later).

The brush synthesis protocol was based on several literature reports.^{56,79} The kinetics of PDMA brush growth at $90 \text{ }^\circ\text{C}$ in DMF are shown in Figure 1 for monomer/catalyst molar ratios

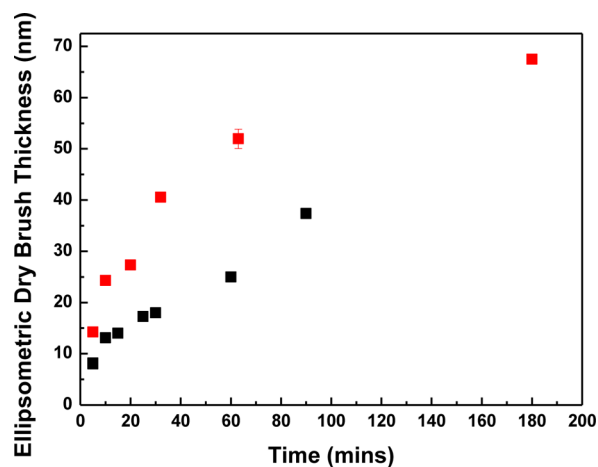


Figure 1. Kinetics of PDMA brush growth via surface-initiated ATRP from silicon wafers immersed in DMF at $90 \text{ }^\circ\text{C}$. Polymerization conditions: (red squares) $[\text{DMA}]:[\text{CuBr}]:[\text{HMTETA}] = 300:1.0:1.50$; (black squares) $[\text{DMA}]:[\text{CuBr}]:[\text{HMTETA}] = 150:1.0:1.50$.

of either 300:1 or 150:1. These brush syntheses were conducted in the absence of any soluble initiator and in each case a monotonic increase in the dry brush thickness was observed, as judged by ellipsometry studies. Mean brush thicknesses of 20–40 nm were typically achieved within 10–30 min for a (preferred) monomer/catalyst molar ratio of 300.

Selective quaternization of these PDMA brushes using various *n*-alkyl iodides was achieved simply by conducting the Menschutkin reaction in *n*-hexane, which is a poor solvent for PDMA. This approach ensures that quaternization is confined to the near-surface of the brush, which allows maximum interaction with the supported lipid bilayer (see Scheme 1). Moreover, it also ensures that the pH-responsive character of the PDMA brush is not lost: control experiments in which quaternization was conducted in THF (a good solvent for the PDMA chains) confirmed that this approach leads to uniform quaternization throughout the brush layer, as expected based on results reported by Bütün and co-workers.⁸⁶ However, this is not desirable, since it suppresses the pH-responsive behavior of the brush (see later). In preliminary studies, we examined

quaternization of PDMA brushes using methyl iodide, *n*-hexyl iodide, *n*-dodecyl iodide, and *n*-stearyl iodide (a.k.a. 1-iodooctadecane). However, only the latter reagent proved to be suitable for the formation of SLBs. Presumably, this is because its C₁₈ alkyl chain is comparable to the hydrophobic tails that make up the lipids used in this work. Thus, all the data presented herein were obtained using 1-iodooctadecane. When reacting the PDMA brush with this reagent in *n*-hexane, the degree of surface quaternization can be assessed using XPS, which has a typical sampling depth of 2–5 nm.⁸⁷ This technique can readily distinguish between cationic (N⁺) and neutral (N⁰) nitrogen atoms in the brush layer, and peak-fitting enables these two species to be quantified. Figure 2 shows

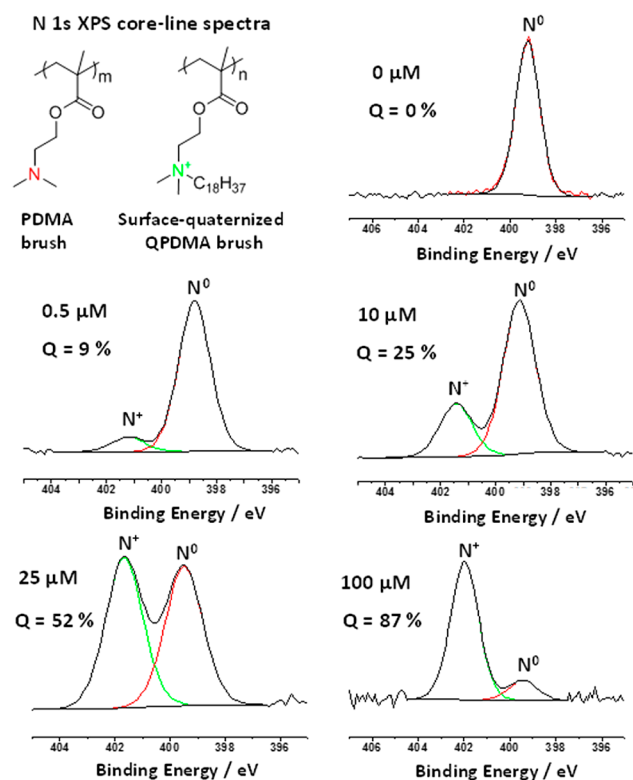


Figure 2. N 1s spectra obtained for PDMA brushes (dry brush thickness = 30–40 nm) on varying the concentration of 1-iodooctadecane in *n*-hexane at 20 °C to achieve partial surface quaternization.

representative N 1s core-line spectra recorded for the pristine PDMA brush and a series of surface-quaternized brushes prepared in *n*-hexane using various concentrations of 1-iodooctadecane. At the highest concentration examined, up to 87% surface quaternization can be achieved within 18 h at 20 °C. Indeed, varying the 1-iodooctadecane concentration provides a convenient means of controlling the final degree of surface quaternization (see Figure 3). There is a monotonic relationship between the degree of surface quaternization and the 1-iodooctadecane concentration used to derivatize the PDMA brush. Moreover, as the degree of surface quaternization is systematically increased from 0 to 50%, the water contact angle (denoted by $\cos \theta$) gradually increases from around 54° to approximately 90°, before becoming constant. This is the result of introducing the relatively hydrophobic 1-octadecyl groups into the brush surface layer (see C 1s core-line spectra shown in Figure S2). Further quaternization experi-

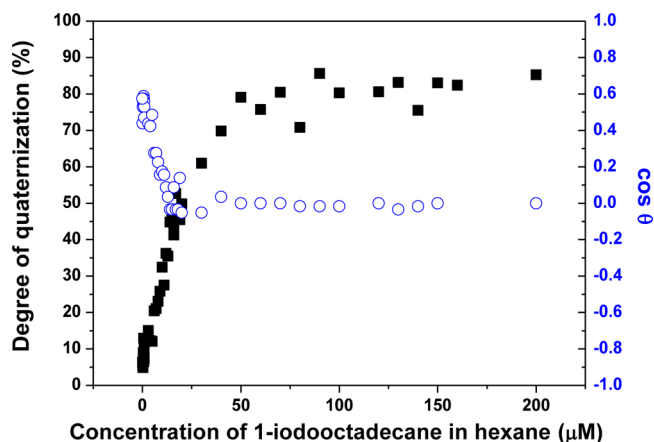


Figure 3. Mean degree of surface quaternization of PDMA brushes (30–40 nm dry thickness) on varying the concentration of 1-iodooctadecane in *n*-hexane at 20 °C, as determined by N 1s XPS analysis (filled squares). Water contact angle data for these surface-quaternized QPDMA brushes are also shown (open circles).

ments were performed to examine whether 100% quaternization could be achieved (see Figures S3 and S4 in the Supporting Information). However, extended reaction times (up to 9 days) and a higher reaction temperature (40 °C) did not allow higher degrees of quaternization to be achieved. Fortunately, for the present work only relatively low degrees of surface quaternization were required to promote surface bilayer formation (see later).

PDMA brushes were also obtained by growing brushes from micropatterned ATRP initiators fabricated by exposure to UV light using a 2000 mesh copper TEM grid as a convenient mask. Such patterned brushes enable the mean brush thickness to be determined via AFM.^{54,75} A representative topographical AFM image and associated height cross-section analysis of a typical micropatterned pH-responsive PDMA brush are shown in Figures 4a and 4b.

Acid titration studies indicate a pK_a of around 7.5 for PDMA, which is a well-known weak polyelectrolyte, in dilute aqueous solution.⁸⁶ On addition of HCl, the pH-responsive PDMA brush chains become protonated; in this highly cationic form they stretch away from the surface, since this provides a mechanism to minimize the strong interchain electrostatic repulsive forces. In contrast, fully quaternized QPDMA is a strong polyelectrolyte that exhibits no pH-responsive character. In principle, partially quaternized QPDMA should exhibit intermediate behavior. However, if quaternization is conducted using a *long chain n*-alkyl halide such as 1-iodooctadecane (as opposed to iodomethane), then strong association between *n*-alkyl groups on adjacent brush chains can occur, leading to the formation of micelle-like structures within the brush layer. These micelles can act as physical cross-links and hence significantly reduce the pH-responsive character of a partially quaternized brush (see later). This problem is much more likely if quaternization occurs uniformly throughout the brush layer, as opposed to being surface-confined (see Scheme 1).

The pH-responsive behavior of a PDMA precursor brush, a *surface-quaternized* QPDMA brush (derivatized in *n*-hexane), and *uniformly quaternized* QPDMA brush (derivatized in THF) is compared in Figure 4c. In each case, the mean dry brush layer thickness was 30–40 nm and each brush was immersed in a series of aqueous buffers ranging from pH 2 to 11.

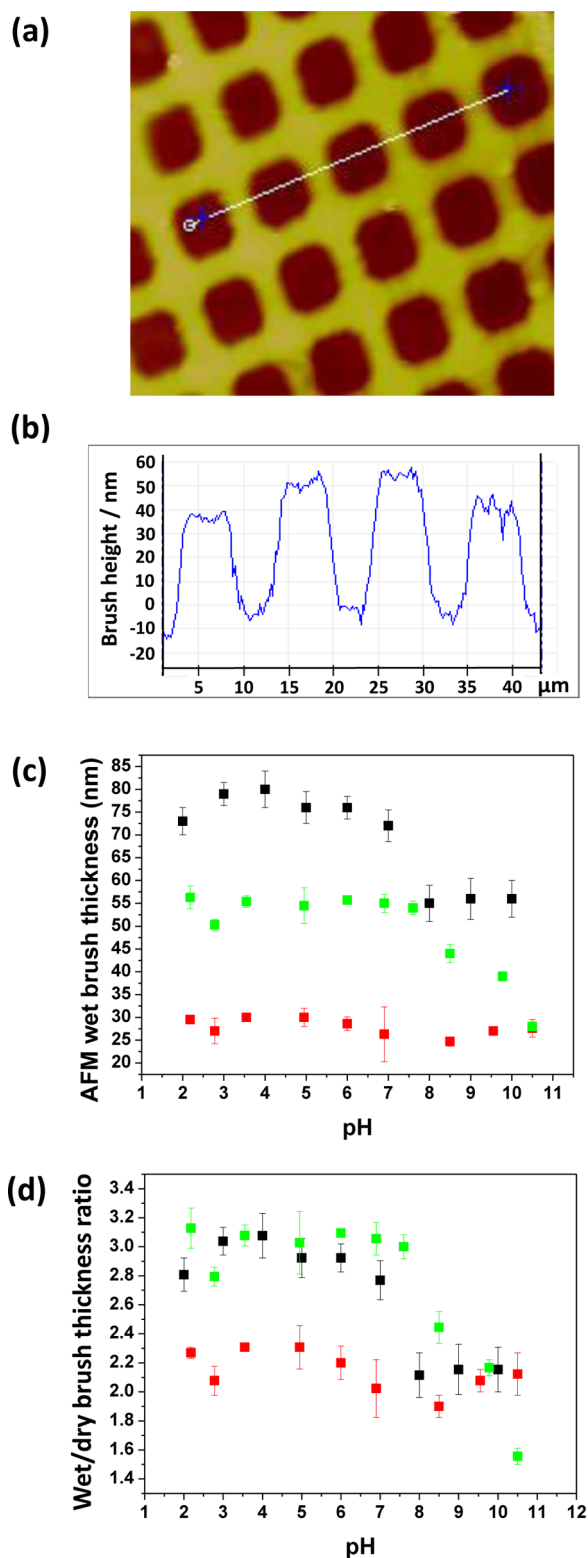


Figure 4. (a) AFM image recorded for a micropatterned PDMA brush and (b) the corresponding cross-section plot obtained by AFM height measurements. *In situ* AFM studies of the pH-responsive behavior of a PDMA brush (black squares, dry brush thickness = 26 nm), a surface-quaternized QPDMA brush (green squares, *n*-hexane, dry brush thickness = 18 nm), and a uniformly quaternized QPDMA brush (red squares, THF, dry brush thickness = 13 nm). The latter two brushes were prepared using 100 μM 1-iodooctadecane at 20 $^{\circ}\text{C}$ in either *n*-hexane or THF. (c) Wet brush thickness vs pH. (d) Normalized brush thickness (or wet/dry brush thickness ratio) vs pH.

As expected, the PDMA precursor brush becomes fully protonated in acidic aqueous solution and attains its maximum swollen thickness of 75–80 nm (see black data set in Figure 4c). In alkaline media, the deprotonated PDMA brush adopts a relatively collapsed conformation of approximately 55 nm thickness. In striking contrast, the *uniformly quaternized* QPDMA brush derivatized in THF exhibited little or no pH-responsive behavior (see red data set in Figure 4c). At first sight, the *surface-quaternized* QPDMA brush derivatized in *n*-hexane appears to exhibit intermediate behavior (see green data set in Figure 4c). However, if the AFM brush height data are normalized to account for the differing dry brush thicknesses (see Figure 4d), then it is clear that there is actually relatively little difference between the PDMA precursor brush and the surface-quaternized PDMA brush. Thus, *surface-confined quaternization is an effective strategy for introducing long-chain *n*-alkyl groups while simultaneously preserving the desired pH-responsive character of the PDMA brush.*

The pH-modulated AFM brush thickness data were corroborated by ellipsometric studies of non-patterned brushes (see Figure 5). When immersed in alkaline buffer (pH > 9), all three brushes exhibited comparable collapsed dimensions (about 1.8–2.0 times the dry brush thickness, see Figure 5b). The mean thickness of a PDMA precursor brush increased up to around 2.55–2.65 times its dry thickness below pH 7. The QPDMA brush derivatized in *n*-hexane produced similar

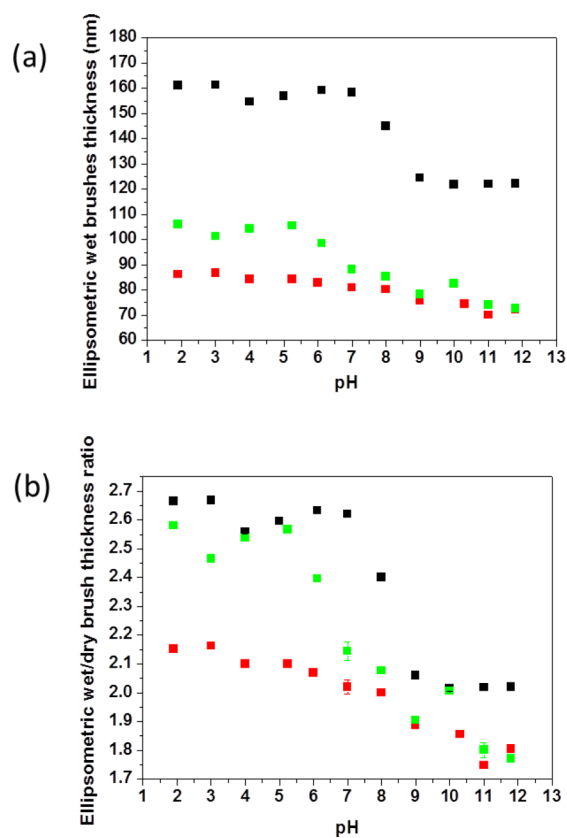


Figure 5. *In situ* ellipsometry studies of the pH-responsive behavior of PDMA (black square, dry brush thickness = 60 nm) and QPDMA (green square, *n*-hexane, dry brush thickness = 41 nm; red square, THF, dry brush thickness = 40 nm) brushes prepared using 100 μM 1-iodooctadecane at 20 $^{\circ}\text{C}$ in either *n*-hexane or THF. (a) Wet brush thickness vs pH. (b) Normalized brush thickness (or wet/dry brush thickness ratio) vs pH.

results, except that a somewhat lower pH ($\text{pH} \sim 5$) was required to achieve the maximum normalized brush height of 2.50–2.60 times the dry brush thickness. This is because quaternization is confined to the (near) surface for this PDMA brush, which therefore minimizes the possibility of physical cross-links within the brush layer. In contrast, the ellipsometric thickness of a *uniformly quaternized* PDMA brush derivatized in THF was relatively insensitive to solution pH from pH 2 to pH 12, as expected. This is attributed to the pendent 1-octadecyl chains forming micelle-like physical cross-links within the brush layer, which hence restrict the chain mobility.

Mixed lipid bilayers (comprising 89.5 mol % POPC, 10 mol % DOPG and 0.5 mol % TR-DHPE fluorescent dye) were formed on *non-quaternized* PDMA precursor brushes with a mean dry brush thickness of 20 nm using the vesicle fusion method, as summarized in Scheme 1 and detailed in the Experimental Section. The diffusion coefficient, D , of the TR-DHPE fluorescent dye within the lipid bilayer was assessed using fluorescence recovery after photobleaching (FRAP) studies (see Figure S5). For a bleach spot size of $96 \mu\text{m}$, the calculated diffusion coefficient and mobile fraction was $2.6 \pm 0.3 \mu\text{m}^2 \text{s}^{-1}$ and $97 \pm 3\%$, respectively. However, such SLBs proved to be unstable after 16 h incubation in buffer at 50°C , since partial delamination of the bilayer from the brush surface was observed (see Figure S6). In addition, adjusting the solution pH to pH 8.7 (or above) also led to SLB instability. This is not unexpected given that the weakly cationic PDMA chains ($\text{p}K_{\text{a}} \sim 7.0^{88}$) become almost neutral at pH 8.7. Thus, there is no longer any electrostatic attraction between the weakly anionic lipid bilayer and the brush chains in mildly alkaline media. In summary, robust SLBs cannot be formed on nonquaternized PDMA precursor brushes by the vesicle fusion method using weakly anionic lipid vesicles. Similarly, only immobilized (pinned) vesicles, rather than mobile SLBs, could be formed on uniformly-quaternized PDMA brushes (see Figure S7).

In principle, surface-quaternized PDMA brushes should produce inherently more stable SLBs, since such brushes retain their cationic character under mildly alkaline conditions. Thus, a PQDMA brush (10 mol % surface quaternization as judged by XPS; 20 nm dry brush thickness) was evaluated for SLB formation using the same POPC/DOPG/TR-DHPE formulation via the vesicle fusion protocol. In this case, robust SLBs were obtained that showed no tendency to undergo delamination in mildly alkaline solution or during incubation at elevated temperature. The diffusion coefficient of the Texas Red fluorescent dye within the lipid bilayer was assessed via FRAP studies (see Figure 6). The two fluorescence microscopy images shown in the inset were recorded immediately following and 6 min after photobleaching using a bleach spot of $\sim 63 \mu\text{m}$ diameter. The experimental data (open circles) and the curve fit (red line) yield a diffusion coefficient and mobile fraction of $2.80 \pm 0.3 \mu\text{m}^2 \text{s}^{-1}$ and $98 \pm 2\%$, respectively.⁸⁹ This D value is comparable to those reported by other workers for supported lipid bilayers formed on alternative polymer brushes.^{58–66} It is also similar to that obtained for the SLB formed on the non-quaternized PDMA precursor brush at neutral pH (see Figure S5), which suggests that 10 mol % quaternization has little or no deleterious effect on the fluidity of the lipid bilayer.^{71,90} Moreover, the surface-confined quaternization strategy described herein preserves the pH-responsive character of the brush, which may be useful for potential applications that require systematic variation of the brush thickness.

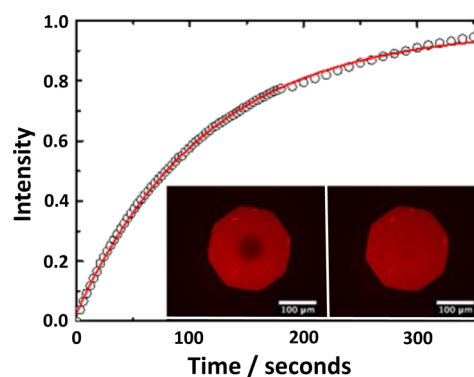


Figure 6. FRAP data obtained for a lipid bilayer formed on a 10% surface-quaternized PDMA brush (dry brush thickness = 20 nm). The open circles represent the experimental data, and the red line is the curve fit obtained using the Axelrod method.⁸⁹ The calculated diffusion coefficient and mobile fraction were $2.8 \pm 0.3 \mu\text{m}^2 \text{s}^{-1}$ and $98 \pm 2\%$, respectively. The vesicle fusion method was used for lipid bilayer formation, and the lipid mixture used to prepare this SLB comprised 89.5 mol % zwitterionic POPC, 10% anionic DOPG, and 0.50 mol % Texas Red-labeled DHPE as a fluorescent probe. Inset images: fluorescence images recorded (left) immediately after bleaching and (right) 6 min after bleaching.

CONCLUSIONS

Surface-confined quaternization of poly(2-dimethylamino)ethyl methacrylate) brushes grown from planar substrates is readily achieved using 1-iodooctadecane by conducting this derivatization in *n*-hexane, which is a bad solvent for the brush chains. This protocol enables the production of robust supported lipid bilayers on the resulting cationic brushes, which retain their pH-responsive character. Moreover, FRAP studies confirm high diffusion coefficients and mobilities, which indicate the formation of high-quality lipid bilayers. A control experiment in which quaternization is conducted using a good solvent for the brush chains (THF) indicate that the pH-responsive character of the original brush layer is not retained under these conditions. Supported lipid bilayers can also be formed on non-quaternized precursor brushes, but such constructs are prone to delamination when immersed in mildly alkaline media, since there is no longer any electrostatic attraction between the brush chains and the lipid bilayer under these conditions. Thus surface-confined quaternization offers important advantages for the design of supported lipid bilayers on polymer brushes.

ASSOCIATED CONTENT

Supporting Information

Surface zeta-potential vs pH curve for a 35 nm PDMA brush; at 40°C , variation of degree of surface quaternization of PDMA brushes with reaction time as judged by XPS, C 1s XPS spectra for QPDMA brushes and PDMA precursor brush obtained using various 1-iodooctadecane concentrations, FRAP data obtained for a lipid bilayer formed on a non-quaternized PDMA brush, and fluorescence images recorded for both this system and a uniformly-quaternized PDMA brush. This material is available free of charge via the Internet at <http://pubs.acs.org>.

AUTHOR INFORMATION

Corresponding Author

*E-mail s.p.arnes@shef.ac.uk (S.P.A.).

Notes

The authors declare no competing financial interest.

ACKNOWLEDGMENTS

EPSRC is thanked for funding this work via a Programme grant (EP/I012060/1).

REFERENCES

- (1) Stuart, M. A. C.; Huck, W. T. S.; Genzer, J.; Mueller, M.; Ober, C.; Stamm, M.; Sukhorukov, G. B.; Szleifer, I.; Tsukruk, V. V.; Urban, M.; Winnik, F.; Zauscher, S.; Luzinov, I.; Minko, S. *Nat. Mater.* **2010**, *9*, 101.
- (2) Liu, F.; Urban, M. W. *Prog. Polym. Sci.* **2010**, *35*, 3.
- (3) Roy, D.; Cambre, J. N.; Sumerlin, B. S. *Prog. Polym. Sci.* **2010**, *35*, 278.
- (4) Chen, T.; Ferris, R.; Zhang, J.; Ducker, R.; Zauscher, S. *Prog. Polym. Sci.* **2010**, *35*, 94.
- (5) Minko, S. *Polym. Rev.* **2006**, *46*, 397.
- (6) Dong, R.; Lindau, M.; Ober, C. K. *Langmuir* **2009**, *25*, 4774.
- (7) Sanjuan, S.; Perrin, P.; Pantoustier, N.; Tran, Y. *Langmuir* **2007**, *23*, 5769.
- (8) Zhou, F.; Huck, W. T. S. *Chem. Commun.* **2005**, 5999.
- (9) Dai, S.; Ravi, P.; Tam, K. C. *Soft Matter* **2008**, *4*, 435.
- (10) Biesalski, M.; Ruhe, J. *Macromolecules* **2002**, *35*, 499.
- (11) Jonas, A. M.; Glinel, K.; Oren, R.; Nysten, B.; Huck, W. T. S. *Macromolecules* **2007**, *40*, 4403.
- (12) Azzaroni, O.; Brown, A. A.; Huck, W. T. S. *Angew. Chem., Int. Ed.* **2006**, *45*, 1770.
- (13) Cheng, N.; Brown, A. A.; Azzaroni, O.; Huck, W. T. S. *Macromolecules* **2008**, *41*, 6317.
- (14) Mizutani, A.; Kikuchi, A.; Yamato, M.; Kanazawa, H.; Okano, T. *Biomaterials* **2008**, *29*, 2073.
- (15) Ionov, L.; Minko, S.; Stamm, M.; Gohy, J. F.; Jerome, R.; Scholl, A. *J. Am. Chem. Soc.* **2003**, *125*, 8302.
- (16) Dunderdale, G.; Fairclough, J. P. A. *Langmuir* **2013**, *29*, 3628.
- (17) Forzani, E. S.; Perez, M. A.; Teijelo, M. L.; Calvo, E. J. *Langmuir* **2002**, *18*, 9867.
- (18) Schmidt, D. J.; Cebeci, F. C.; Kalcioğlu, Z. I.; Wyman, S. G.; Ortiz, C.; Van Vliet, K. J.; Hammond, P. T. *ACS Nano* **2009**, *3*, 2207.
- (19) Mendes, P. M. *Chem. Soc. Rev.* **2008**, *37*, 2512.
- (20) Alexander, C.; Shakesheff, K. M. *Adv. Mater.* **2006**, *18*, 3321.
- (21) Bajpai, A. K.; Shukla, S. K.; Bhanu, S.; Kankane, S. *Prog. Polym. Sci.* **2008**, *33*, 1088.
- (22) Raviv, U.; Giasson, S.; Kampf, N.; Gohy, J. F.; Jerome, R.; Klein, J. *Nature* **2003**, *425*, 163.
- (23) Tam, T. K.; Ornatka, M.; Pita, M.; Minko, S.; Katz, E. *J. Phys. Chem. C* **2008**, *112*, 8438.
- (24) Alonzi, M.; Lanari, D.; Marrocchi, A.; Petrucci, C.; Vaccaro, L. *RSC Adv.* **2013**, *3*, 23909.
- (25) Brunetti, F. G.; Kumar, R.; Wudl, F. *J. Mater. Chem.* **2010**, *20*, 2934.
- (26) Barbey, R.; Lavanant, L.; Paripovic, D.; Schuwer, N.; Sugnaux, C.; Tugulu, S.; Klok, H. A. *Chem. Rev.* **2009**, *109*, 5437.
- (27) Husseman, M.; Malmstrom, E. E.; McNamara, M.; Mate, M.; Mecerreyes, D.; Benoit, D. G.; Hedrick, J. L.; Mansky, P.; Huang, E.; Russell, T. P.; Hawker, C. J. *Macromolecules* **1999**, *32*, 1424.
- (28) Matyjaszewski, K.; Miller, P. J.; Shukla, N.; Immaraporn, B.; Gelman, A.; Luokala, B. B.; Siclován, T. M.; Kickelbick, G.; Vallant, T.; Hoffmann, H.; Pakula, T. *Macromolecules* **1999**, *32*, 8716.
- (29) Edmondson, S.; Osborne, V. L.; Huck, W. T. S. *Chem. Soc. Rev.* **2004**, *33*, 14.
- (30) Edmondson, S.; Armes, S. P. *Polym. Int.* **2009**, *58*, 307.
- (31) Carlmark, A.; Malmstrom, E. *J. Am. Chem. Soc.* **2002**, *124*, 900.
- (32) Pyun, J.; Kowalewski, T.; Matyjaszewski, K. *Macromol. Rapid Commun.* **2003**, *24*, 1043.
- (33) Chen, X. Y.; Armes, S. P. *Adv. Mater.* **2003**, *15*, 1558.
- (34) Perruchot, C.; Khan, M. A.; Kamitsi, A.; Armes, S. P.; von Werne, T.; Patten, T. E. *Langmuir* **2001**, *17*, 4479.
- (35) Zhao, Y.; Perrier, S. *Macromolecules* **2006**, *39*, 8603.
- (36) Hawker, C. J.; Bosman, A. W.; Harth, E. *Chem. Rev.* **2001**, *101*, 3661.
- (37) Matyjaszewski, K.; Xia, J. H. *Chem. Rev.* **2001**, *101*, 2921.
- (38) Moad, G.; Rizzardo, E.; Thang, S. H. *Aust. J. Chem.* **2005**, *58*, 379.
- (39) Parnell, A. J.; Martin, S. J.; Jones, R. A. L.; Vasilev, C.; Crook, C. J.; Ryan, A. J. *Soft Matter* **2009**, *5*, 296.
- (40) Parnell, A. J.; Martin, S. J.; Dang, C. C.; Geoghegan, M.; Jones, R. A. L.; Crook, C. J.; Howse, J. R.; Ryan, A. J. *Polymer* **2009**, *50*, 1005.
- (41) Iwata, H.; Hirata, I.; Ikada, Y. *Macromolecules* **1998**, *31*, 3671.
- (42) Zhou, F.; Shu, W. M.; Welland, M. E.; Huck, W. T. S. *J. Am. Chem. Soc.* **2006**, *128*, 5326.
- (43) Sun, J.-T.; Hong, C.-Y.; Pan, C.-Y. *J. Phys. Chem. C* **2010**, *114*, 12481.
- (44) Ionov, L.; Houbenov, N.; Sidorenko, A.; Stamm, M.; Minko, S. *Adv. Funct. Mater.* **2006**, *16*, 1153.
- (45) Schuwer, N.; Klok, H. A. *Langmuir* **2011**, *27*, 4789.
- (46) Ding, S. J.; Floyd, J. A.; Walters, K. B. *J. Polym. Sci., Part A: Polym. Chem.* **2009**, *47*, 6552.
- (47) Moglianetti, M.; Webster, J. R. P.; Edmondson, S.; Armes, S. P.; Titmuss, S. *Langmuir* **2010**, *26*, 12684.
- (48) Fielding, L. A.; Edmondson, S.; Armes, S. P. *J. Mater. Chem.* **2011**, *21*, 11773.
- (49) Barbey, R.; Klok, H.-A. *Langmuir* **2010**, *26*, 18219.
- (50) Topham, P. D.; Howse, J. R.; Crook, C. J.; Parnell, A. J.; Geoghegan, M.; Jones, R. A. L.; Ryan, A. J. *Polym. Int.* **2006**, *55*, 808.
- (51) Edmondson, S.; Vo, C. D.; Armes, S. P.; Unali, G. F. *Macromolecules* **2007**, *40*, 5271.
- (52) Stratakis, E.; Mateescu, A.; Barberoglou, M.; Vamvakaki, M.; Fotakis, C.; Anastasiadis, S. H. *Chem. Commun.* **2010**, *46*, 4136.
- (53) Thomassin, J.-M.; Lenoir, S.; Riga, J.; Jerome, R.; Detrembleur, C. *Biomacromolecules* **2007**, *8*, 1171.
- (54) Alswieleh, A. M.; Cheng, N.; Leggett, G. J.; Armes, S. P. *Langmuir* **2014**, *30*, 1391.
- (55) Murata, H.; Koepsel, R. R.; Matyjaszewski, K.; Russell, A. J. *Biomaterials* **2007**, *28*, 4870.
- (56) Cheng, Z. P.; Zhu, X. L.; Shi, Z. L.; Neoh, K. G.; Kang, E. T. *Ind. Eng. Chem. Res.* **2005**, *44*, 7098.
- (57) Dong, R.; Molloy, R. P.; Lindau, M.; Ober, C. K. *Biomacromolecules* **2010**, *11*, 2027.
- (58) Cassier, T.; Sinner, A.; Offenhauser, A.; Mohwald, H. *Colloids Surf., B* **1999**, *15*, 215.
- (59) Fang, N.; Tan, W. J.; Leong, K. W.; Mao, H. Q.; Chan, V. *Colloids Surf., B* **2005**, *42*, 245.
- (60) Fischlechner, M.; Zaulig, M.; Meyer, S.; Estrela-Lopis, I.; Cuellar, L.; Irigoyen, J.; Pescador, P.; Brumen, M.; Messner, P.; Moya, S.; Donath, E. *Soft Matter* **2008**, *4*, 2245.
- (61) Kaufmann, M.; Jia, Y.; Werner, C.; Pompe, T. *Langmuir* **2011**, *27*, 513.
- (62) Kugler, R.; Knoll, W. *Bioelectrochemistry* **2002**, *56*, 175.
- (63) Renner, L.; Osaki, T.; Chiantia, S.; Schwille, P.; Pompe, T.; Werner, C. *J. Phys. Chem. B* **2008**, *112*, 6373.
- (64) Santonicola, M. G.; Memesa, M.; Meszynska, A.; Ma, Y.; Vancso, G. J. *Soft Matter* **2012**, *8*, 1556.
- (65) Smith, E. A.; Coym, J. W.; Cowell, S. M.; Tokimoto, T.; Hruby, V. J.; Yamamura, H. I.; Wirth, M. J. *Langmuir* **2005**, *21*, 9644.
- (66) Tang, Y.; Wang, Z.; Xiao, J.; Yang, S.; Wang, Y. J.; Tong, P. *J. Phys. Chem. B* **2009**, *113*, 14925.
- (67) Sackmann, E. *Science* **1996**, *271*, 43.
- (68) Wagner, M. L.; Tamm, L. K. *Biophys. J.* **2000**, *79*, 1400.
- (69) Albertorio, F.; Diaz, A. J.; Yang, T. L.; Chapa, V. A.; Kataoka, S.; Castellana, E. T.; Cremer, P. S. *Langmuir* **2005**, *21*, 7476.
- (70) Munro, J. C.; Frank, C. W. *Langmuir* **2004**, *20*, 10567.
- (71) Mashaghi, S.; van Oijen, A. M. *Biotechnol. Bioeng.* **2014**, *111*, 2076.
- (72) Goennenwein, S.; Tanaka, M.; Hu, B.; Moroder, L.; Sackmann, E. *Biophys. J.* **2003**, *85*, 646.

- (73) Elender, G.; Kuhner, M.; Sackmann, E. *Biosens. Bioelectron.* **1996**, *11*, 565.
- (74) El-Khoury, R. J.; Bricarello, D. A.; Watkins, E. B.; Kim, C. Y.; Miller, C. E.; Patten, T. E.; Parikh, A. N.; Kuhl, T. L. *Nano Lett.* **2011**, *11*, 2169.
- (75) Alswieleh, A. M.; Cheng, N.; Canton, I.; Ustbas, B.; Xue, X.; Ladmiral, V.; Xia, S. J.; Ducker, R. E.; El Zubir, O.; Cartron, M. L.; Hunter, C. N.; Leggett, G. J.; Armes, S. P. *J. Am. Chem. Soc.* **2014**, *136*, 9404.
- (76) Blakeston, A. A.; Heath, G. R.; Roth, J. S.; Bao, P.; Cheng, N.; Armes, S. P.; Leggett, G. J.; Bushby, R. J.; Evans, S. D. *Langmuir* **2014**, DOI: 10.1021/la504163s.
- (77) Plamper, F. A.; Schmalz, A.; Penott-Chang, E.; Drechsler, M.; Jusufi, A.; Ballauff, M.; Muller, A. H. E. *Macromolecules* **2007**, *40*, 5689.
- (78) Huang, J. Y.; Murata, H.; Koepsel, R. R.; Russell, A. J.; Matyjaszewski, K. *Biomacromolecules* **2007**, *8*, 1396.
- (79) Yu, W. H.; Kang, E. T.; Neoh, K. G.; Zhu, S. P. *J. Phys. Chem. B* **2003**, *107*, 10198.
- (80) Brian, A. A.; McConnell, H. M. *Proc. Natl. Acad. Sci. U. S. A.* **1984**, *81*, 6159.
- (81) Alang Ahmad, S. A.; Leggett, G.; Hucknall, A.; Chilkoti, A. *Biointerphases* **2011**, *6*, 8.
- (82) Janssen, D.; De Palma, R.; Verlaak, S.; Heremans, P.; Dehaen, W. *Thin Solid Films* **2006**, *515*, 1433.
- (83) Alang Ahmad, S. A.; Hucknall, A.; Chilkoti, A.; Leggett, G. J. *Langmuir* **2010**, *26*, 9937.
- (84) Bao, P.; Cheetham, M. R.; Roth, J. S.; Blakeston, A. C.; Bushby, R. J.; Evans, S. D. *Anal. Chem.* **2012**, *84*, 10702.
- (85) Edmondson, S.; Nguyen, N. T.; Lewis, A. L.; Armes, S. P. *Langmuir* **2010**, *26*, 7216.
- (86) Bütin, V.; Armes, S. P.; Billingham, N. C. *Macromolecules* **2001**, *34*, 1148.
- (87) Cumpson, P. J. *J. Electron Spectrosc. Relat. Phenom.* **1995**, *73*, 25.
- (88) Bütin, V.; Armes, S. P.; Billingham, N. C. *Polymer* **2001**, *42*, 5993.
- (89) Axelrod, D.; Koppel, D. E.; Schlessinger, J.; Elson, E.; Webb, W. W. *Biophys. J.* **1976**, *16*, 1055.
- (90) Deverall, M. A.; Garg, S.; Ludtke, K.; Jordan, R.; Ruhe, J.; Naumann, C. A. *Soft Matter* **2008**, *4*, 1899.